

Helix–Turn–Helix Motifs in Unsolvated Peptides

David T. Kaleta and Martin F. Jarrold*

Department of Chemistry, Indiana University, 800 East Kirkwood Avenue, Bloomington, Indiana 47405

Received March 24, 2003; E-mail: mfj@indiana.edu

The aggregation of secondary structure elements into motifs provides proteins with functional sites and the building blocks for the development of larger structures (domains) that ultimately define a protein's distinct three-dimensional shape.¹ The helix–turn–helix, or α -helical hairpin, motif is one of the simplest found in nature, variants of which form the DNA-binding² and calcium-binding motifs.³ Here we report studies of the conformations of the peptide Ac-A₁₄KG₃A₁₄K + 2H⁺ (Ac = acetyl, A = alanine, K = lysine, and G = glycine) which was designed to adopt a model helix–turn–helix motif in the gas phase. Experimentally, we find three distinct geometries for this peptide, the dominant being an arrangement with two helical alanine sections, linked by a glycine loop, in an antiparallel coiled-coil arrangement, see Figure 1a. When the temperature is raised above 360 K the helices uncouple and become uncorrelated while the loop region randomizes. We have determined ΔH° and ΔS° for this coupling \rightleftharpoons uncoupling transition, which represents the simplest step in the aggregation of secondary structure elements.

Studies of unsolvated peptides provide information about the intramolecular interactions important in protein folding.^{4–6} These studies are particularly relevant to membrane proteins, where our knowledge is much less well developed than for globular proteins. In the present work we have used ion mobility measurements to probe the conformations of model peptides. The mobility of an ion in a weak electric field provides a measure of its average collision cross section. Small, compact structures undergo fewer collisions with the buffer gas and travel more rapidly than larger structures. Structural assignments are made by comparing cross sections obtained from the experiments to those determined from molecular dynamics simulations. The Ac-A₁₄KG₃A₁₄K + 2H⁺ peptide was designed to form two helices connected by a glycine loop. Unsolvated Ac-A₁₄K + H⁺ peptides are known to form helices.⁷ The helical conformation is stabilized by favorable interactions between the charge and the helix dipole and by capping the C-terminus with the protonated lysine side chain.^{8–10} Glycine was chosen to make the G₃ loop linking the two helical A₁₄K units together because it has a low helix propensity (both in solution and in the gas phase).^{11,12}

Ac-A₁₄KG₃A₁₄K was synthesized using an Applied Biosystems Model 433A peptide synthesizer with *FastMoc* chemistry. Mobility measurements were performed on custom-built apparatus that consists of an electrospray source, a temperature-variable drift tube, a quadrupole mass spectrometer, and a detector.¹³ Drift time distributions (DTDs) are measured by injecting 100 μ s pulses of ions into the drift tube and recording their arrival time distributions at the detector. DTDs recorded for Ac-A₁₄KG₃A₁₄K + 2H⁺ are shown in Figure 1. At low temperatures there are three major peaks (the small peak at around 6.8 ms is an artifact). The peak with the longest drift time disappears at around 230 K. Two peaks are present at room temperature, but at around 350 K they coalesce into a single peak which then starts to move to longer drift times as the temperature is raised further.

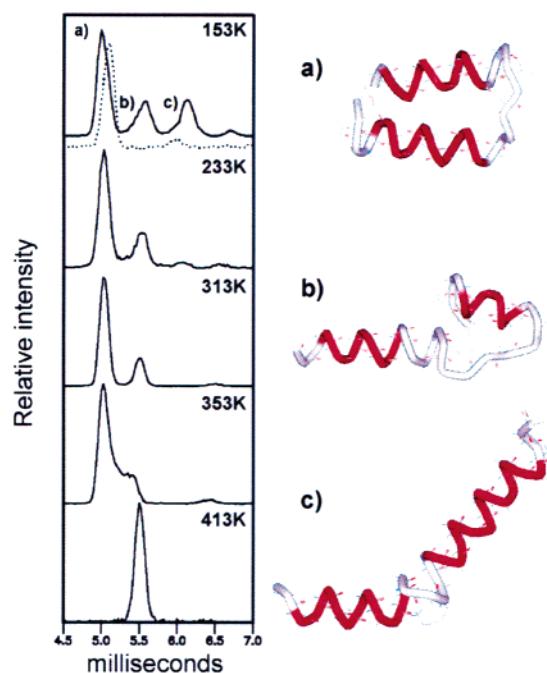


Figure 1. Drift time distributions recorded for Ac-A₁₄KG₃A₁₄K + 2H⁺ (solid lines) and Ac-A₁₄KSar₃A₁₄K + 2H⁺ (dotted line) and the conformations derived from molecular dynamics simulations that are believed to be responsible for the three main features observed in the experimental distributions: (a) coiled-coil, (b) exchanged lysine, and (c) extended helical conformation. The images were produced using ViewerLite (Accelrys, Inc., San Diego, CA). The red regions are α -helical.

Molecular dynamics (MD) simulations were performed to assign the features in the DTDs to specific conformations. The simulations were carried out with the MACSIMUS molecular modeling suite,¹⁴ using the CHARMM (21.3) force field¹⁵ and a dielectric constant of 1.0 (which is appropriate for small unsolvated peptides). Average cross sections were obtained from the final 35 ps of each simulation using an empirical correction to the exact hard spheres scattering model.¹⁶ The average cross section is expected to be within 2% of the experimentally determined cross section if the conformation is correct. A large number of constant temperature and simulated annealing¹⁷ runs were performed, starting from a wide range of different conformations (including fully collinear helix, fully linear string, half-helix and half-linear string, and coiled-coil). The charges were located on the lysine side chains.

Two major groups of conformations emerged from the simulations: a coiled-coil, an example of which is shown in Figure 1a, and an extended helical conformation represented by Figure 1c. The coiled-coil has two helical sections aligned antiparallel. This conformation is stabilized by favorable electrostatic interactions between the helices and by interactions between the carboxylic acid group at the C-terminus and the amide group(s) at the N-terminus. In the simulations, the interhelical angle fluctuates between 0° and

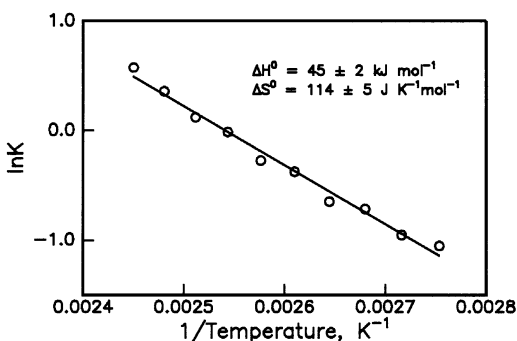


Figure 2. Plot of $\ln K$ against $1/T$ for the coupling \rightleftharpoons uncoupling equilibrium for the Ac-A₁₄KG₃A₁₄K + 2H⁺ coiled-coil.

20° on a ps time scale. This range of angles is consistent with the “ridges in grooves” model of coiled-coils.¹⁸ The other major group of conformations found in the simulations is the extended helix shown in Figure 1c. The extended helix is distorted near its midpoint by the lysine side chain. The coiled-coil is around 30 kJ mol⁻¹ lower in energy than the extended helix in the simulations and has a calculated cross section that matches the measured value for the dominant feature in the DTDs. The cross section for the extended conformation is close to matching that for the feature with the longest drift time (the one that disappears at around 230 K). Another plausible arrangement is an un-kinked extended helix generated by shifting a proton from the middle lysine to the backbone carbonyl group nearest the C-terminus. However, the cross section for this arrangement is in slightly worse agreement with experiment.

The MD simulations did not reveal any low-energy conformations that could account for the middle feature in the DTDs (the one that survives to around 350 K). What we believe to be the most likely assignment for this feature is shown in Figure 1b. This structure has exchanged lysines: the lysine from one A₁₄K unit interacts with the C-terminus of the other. A high temperature, ≥ 600 K, is required to form this conformation in the simulations, and once formed, temperatures ≥ 800 K are required to disrupt it (these temperatures are artificially elevated by the short time scale of the simulations). The exchanged structure is around 50 kJ mol⁻¹ higher in energy than the coiled-coil (at least partly because of unfavorable electrostatic interactions). The most likely scenario is that some peptides become trapped in this high-energy conformation either during the desolvation process or when the ions are collisionally heated as they enter the drift tube. Once formed, relatively high temperatures are required to anneal them away. The exchanged-lysines motif has been invoked to explain the formation of some noncovalent peptide complexes.¹⁹

The assignments described above were confirmed by studies of Ac-A₁₄KSar₃A₁₄K + 2H⁺ (Sar = sarcosine; glycine with a methyl group blocking the amide nitrogen so that it cannot form helical hydrogen bonds). For the sarcosine analogue, the coiled-coil and extended conformation (which is less abundant than for Ac-A₁₄KG₃A₁₄K + 2H⁺) are present but the exchanged conformation is missing (see dotted line in Figure 1). This is consistent with MD simulations for Ac-A₁₄KSar₃A₁₄K + 2H⁺, where the exchanged conformation was not spontaneously generated at elevated temperatures, and when forced into this conformation it promptly annealed away at a relatively low temperature. Coiled-coils and extended conformations were found in the Ac-A₁₄KSar₃A₁₄K + 2H⁺ simulations, and their cross sections closely match those for the two features evident for this peptide in Figure 1.

At temperatures above around 360 K there is only a single relatively narrow peak in the DTD which shifts to a larger cross

section with increasing temperature. This behavior suggests that the helices in the coiled-coil are becoming uncoupled and spending part of their time in a random orientation relative to each other. The position of the measured peak with respect to the positions expected for the coiled-coil and the average uncoupled arrangement provides a measure of the amount of time spent in each configuration, which is equivalent to the equilibrium constant. Equilibrium constants determined in this way for the coupling \rightleftharpoons uncoupling transition for the Ac-A₁₄KG₃A₁₄K + 2H⁺ coiled-coil are shown in Figure 2, where $\ln K$ is plotted against $1/T$. The slope of this van't Hoff plot yields $\Delta H^\circ = -45$ kJ mol⁻¹ and the intercept yields $\Delta S^\circ = 114$ J K⁻¹ mol⁻¹. $-\Delta H^\circ$ is essentially the enthalpy change for docking the two helices together, the value of 45 kJ mol⁻¹ found here is mainly due to electrostatic and van der Waals interactions because there are no specific chemical interactions binding the helices together in this peptide. ΔS° is essentially the entropy change for freeing up the glycine loop. The backbone entropy of glycine has previously been estimated to be around 28 J K⁻¹ mol⁻¹,²⁰ $3 \times 28 = 84$ J K⁻¹ mol⁻¹, which is reasonably close to the $\Delta S^\circ = 114$ J K⁻¹ mol⁻¹ determined here. The discrepancy may be due to fraying at the ends of the helix. The approach described here provides a framework to dissect the interactions responsible for the stability of the helix–turn–helix motif by making substitutions along the lengths of the helices and to the loop region. We intend to explore these avenues.

Acknowledgment. We wish to thank Jiri Kolafa for the use of his MACSIMUS molecular modeling programs. We gratefully acknowledge the support of the National Institutes of Health.

References

- (1) Branden, C.; Tooze, J. *Introduction to Protein Structure*, 2nd ed.; Garland: New York, 1999.
- (2) Anderson, W. F.; Ohlendorf, W. H.; Takeda, Y.; Mathew, B. W. *Nature* **1981**, *290*, 754–758.
- (3) Kretsinger, R. H. Nockolds, C. E. *J. Biol. Chem.* **1973**, *248*, 3313–3326.
- (4) Dill, K. A. *Biochemistry* **1990**, *29*, 7133–7155.
- (5) Jarrold, M. F. *Annu. Rev. Phys. Chem.* **2000**, *51*, 179–207.
- (6) For examples of studies of unsolvated peptides and proteins, see: Suckau, D.; Shi, Y.; Beu, S. C.; Senko, M. W.; Quinn, J. P.; Wampler, F. M.; McLafferty, F. W. *Proc. Natl. Acad. Sci. U.S.A.* **1993**, *90*, 790–793. Campbell, S.; Rodgers, M. T.; Marzluff, E. M.; Beauchamp, J. L. *J. Am. Chem. Soc.* **1995**, *117*, 12840–12854. Schnier, P. D.; Price, W. D.; Jockusch, R. A.; Williams, E. R. *J. Am. Chem. Soc.* **1996**, *118*, 7178–7189. Kaltashov, I. A.; Fenselau, C. *Proteins: Struct. Func. Genet.* **1997**, *27*, 165–170. Valentine, S. J.; Clemmer, D. E. *J. Am. Chem. Soc.* **1997**, *119*, 3558–3566. Wyttenbach, T.; Bushnell, J. E.; Bowers, M. T. *J. Am. Chem. Soc.* **1998**, *120*, 5098–5103. Artega, G. A.; Velázquez, I.; Reimann, C. T.; Tapia, O. *Phys. Rev. E* **1999**, *59*, 5981–5986. Schaaff, T. G.; Stephenson, J. L.; McLuckey, S. L. *J. Am. Chem. Soc.* **1999**, *121*, 8907–8919. Ruotolo, B. T.; Verbeck, G. F.; Thomson, L. M.; Gillig, K. J.; Russell, D. H. *J. Am. Chem. Soc.* **2002**, *124*, 4214–4215.
- (7) Hudgins, R. R.; Ratner, M. A.; Jarrold, M. F. *J. Am. Chem. Soc.* **1998**, *120*, 12974–12975.
- (8) Experimental results indicate that the lysine side chain is protonated in these peptides (see, for example, ref 6).
- (9) Presa, L. G.; Rose, G. D. *Science* **1988**, *240*, 1632–1641.
- (10) Seale, J. W.; Srinivasan, R.; Rose, G. D. *Protein Sci.* **1994**, *3*, 1741–1745.
- (11) Chakrabarty, A.; Baldwin, R. L. *Adv. Prot. Chem.* **1995**, *46*, 141–176.
- (12) Hudgins, R. R.; Jarrold, M. F. *J. Phys. Chem. B* **2000**, *104*, 2154–2158.
- (13) Kinnear, B. S.; Hartings, M. R.; Jarrold, M. F. *J. Am. Chem. Soc.* **2001**, *123*, 5660–5667.
- (14) <http://www.icpf.cas.cz/jiri/macsimus/default.htm>.
- (15) Brooks, B. R.; Bruccoleri, R. E.; Olafson, B. D.; States, D. J.; Swaminathan, S.; Karplus, M. *J. Comput. Chem.* **1983**, *4*, 187–217.
- (16) Kinnear, B. S.; Kaleta, D. T.; Kohtani, M.; Hudgins, R. R.; Jarrold, M. F. *J. Am. Chem. Soc.* **2000**, *122*, 9243–9256.
- (17) Kirkpatrick, S.; Gelatt, C. D., Jr.; Vecchi, M. P. *Science* **1983**, *220*, 671–680.
- (18) Chothia, C.; Levitt, M.; Richardson, D. *Proc. Natl. Acad. Sci. U.S.A.* **1977**, *74*, 4130–4134.
- (19) Kaleta, D. T.; Jarrold, M. F. *J. Am. Chem. Soc.* **2002**, *124*, 1154–1155. Kaleta, D. T.; Jarrold, M. F. *J. Phys. Chem. A* **2002**, *106*, 9655–9664.
- (20) Zhang, C.; Cornette, J. L.; Delisi, C. *Protein Sci.* **1997**, *6*, 1057–1064.

JA0353006